Available online at www.sciencedirect.com
ScienceDirect
Journal of the European Ceramic Society 31 (2011) 1103–1111
www.elsevier.com/locate/jeurceramsoc

Original Article

Densification behavior and properties of hot-pressed ZrC ceramics with Zr and graphite additives

Xin-Gang Wang, Wei-Ming Guo, Yan-Mei Kan, Guo-Jun Zhang *, Pei-Ling Wang

State Key Laboratory of High Performance Ceramics and Superfine Microstructures, Shanghai Institute of Ceramics, Shanghai 200050, China

Received 5 November 2010; received in revised form 16 December 2010; accepted 10 January 2011
Available online 4 February 2011

Abstract

Densifications of hot-pressed ZrC ceramics with Zr and graphite additives were studied at 1800–2000 °C. ZrC with 8.94 wt% Zr additive (named ZC10) sintered at 1900–2000 °C achieved higher relative densities (>98.4%) than that of additive-free ZrC (<83%). The densification improvement was attributed to the formation of non-stoichiometric $ZrC_{0.9}$, whereas there had rapid grain growth with grain size about 50–100 μm in ZC10. By adding co-doped additive of Zr plus C and adjusting the molar ratio of Zr/C, ZrC with co-doped additives with Zr/C molar ratio at 1:2 (named ZC12), ZrC ceramics with both high relative density (98.4%) and fine microstructures (grain size about 5–10 μm) were obtained at 1900–2000 °C. Effect of formation of non-stoichiometric ZrC_{1-x} on densification of ZrC was discussed. The Vickers hardness and indentation toughness of ZC10 and ZC12 samples sintered at 1900 °C were 17.8 GPa and 3.0 MPa $m^{1/2}$, 16.2 GPa and 4.7 MPa $m^{1/2}$, respectively.

Keywords: Sintering; Carbides; Mechanical properties; Refractories

1. Introduction

Refractory zirconium, hafnium and tantalum carbides exhibit considerable potential for ultra-high-temperature applications duo to their high melting point, high hardness, good thermal shock resistance, and solid-state phase stability.[1,2] The density of stoichiometric ZrC (6.64 g cm^{-3}) is much lower than those of other refractory carbides such as HfC (12.7 g cm^{-3}), TaC (14.8 g cm^{-3}) and WC (15.6 g cm^{-3}),[3] so ZrC could be a good potential material for structure component used in next-generation rocket engines and hypersonic spacecraft.[4,5] In addition, in the frame work of the Generation-IV nuclear energy system, ZrC is one of the possible inert matrix materials for gas-cooled fast reactor (GFR) fuel and potential fuel coating material for high-temperature gas-cooled reactor (HTGR) fuel due to its resistance to corrosion by fission products and neutronic properties.[6,7]

However, ZrC is also characterized by its poor sinterability, mainly due to its strong covalent bond characteristics and low self-diffusion coefficient, analogous to that of other carbides such as HfC, SiC, and B_4C. In this context, pressure-assisted techniques and high sintering temperatures are generally applied to get dense ZrC bodies.[8,9] For example, without any sintering aids, ZrC ceramics with relative density ranging from 94% to 97% were obtained by hot-pressing under 30–40 MPa at temperatures higher than 2200 °C.[10,11] To reduce the sintering temperature required for densification, various metallic, oxide, and non-oxide additives have been chosen as sintering aids. It was found that the introduction of metallic additives such as Mo[12] and Nb[13] into ZrC could promote densification by forming liquid phase. However the retained metal phase in the grain boundary would result in poor corrosion resistance and decrease material strength at high temperature. Inorganic additives, like ZrO_2[14] and $MoSi_2$[8] have also been used to improve the densification of ZrC. In the case of ZrO_2, a ZrC_xO_y solution formed by the reaction of ZrC matrix with ZrO_2 promoted the densification. The increase in fracture toughness and strength of the sintered product was attributed to the presence of tetragonal phase ZrO_2.[14] While in the case of $MoSi_2$, the formation of a liquid phase might enhance the densification process.[8] In addition to the additive approach that is commonly used to produce dense ZrC-based ceramics, reactive hot pressing (RHP) is another way to obtain high-dense ceramics, which has an advantage of producing ceramics at reduced temperatures compared

* Corresponding author. Tel.: +86 21 52411080; fax: +86 21 52413122.
E-mail address: gjzhang@mail.sic.ac.cn (G.-J. Zhang).

0955-2219/$ – see front matter © 2011 Elsevier Ltd. All rights reserved.
doi:10.1016/j.jeurceramsoc.2011.01.005

with non-reactive processes,[15,16] Nachiappan et al. carried out the synthesis and densification of ZrC by RHP of Zr and C powders.[17] The results showed that nearly fully dense material with fine grains could be prepared at temperature as low as 1200 °C with C/Zr ~0.67.

For non-stoichiometric compound ZrC_{1-x}, the sinterability was influenced by the carbon vacancy concentration in the composition, and the relative density ZrC_{1-x} ceramics was increased from 91% to 97.8% by hot pressing at 2300 °C for 5 min when x was changed from 0 to 0.35.[18] The results indicated that the densification of carbon deficient compositions can be realized at lower temperature than the composition close to stoichiometry. The increase in carbon diffusivity as well as a decrease in the critical resolved flow stress in non-stoichiometry compositions could be responsible for the pronounced densification.[19] In addition, it was reported that mass transport effects were composition dependent, carbides such as TiC and ZrC with high carbon-vacancy concentration usually had rapid sintering and excessive grain growth.[20]

The aim of the present work was to improve the sinterability of commercial ZrC powders by using Zr and graphite additives. Firstly, the densification behavior of ZrC ceramics by addition of Zr was studied. Then the densification of the ZrC ceramics co-doped with Zr and graphite was investigated and compared with the Zr-doped one. It was kept in mind that the formation of non-stoichiometric compound ZrC_{1-x} with high carbon vacancy concentration should be avoided to refrain from the abnormal grain growth during sintering. The microstructures and mechanical properties of the sintered ceramics were also characterized.

2. Experimental

ZrC (lattice parameter 4.6948 Å, particle size 2–5 μm, purity 95%, impurities include Hf 3.0 wt%, Ti 0.13 wt%, Nb 0.05 wt%, O 0.78 wt%, Mg 0.1 wt%, High Purity Chemical Institute Co. Ltd., Saitama, Japan), Zr (particle size <25 μm, purity >98%, Beijing Mountain Technical Development Center for Nonferrous Metals, Beijing, China) and graphite powders (particle size 2–5 μm, 99% purity, Shanghai Colloid Chemistry Company, Shanghai, China) were used as the starting materials. The measured lattice parameter of raw ZrC powder is 4.6948 Å, which is close to the data (4.694 Å) of nearly stoichiometric ZrC given by JCPDS Card 65-0332 and reported value,[8] implying that the ZrC raw powder is close to the stoichiometric one. Zr powder was milled in acetone for 8 h using Si_3N_4 media by planetary milling to reduce the particle size. ZrC powders together with additives were mixed in ethanol for 24 h using Si_3N_4 balls as media. When mixing ZrC with Zr and graphite additives, Zr and graphite was mixed for 8 h firstly in order to increase the contact of additives, then ZrC was added into the additives mixture to mix for 24 h further. A rotary evaporator was used to dry the obtained slurries at 60 °C. The raw material compositions used in the present work are listed in Table 1, in which the samples without additive, with addition of Zr (8.94 wt%), and with co-doped by Zr plus C at the Zr/C molar ratios of 1:1 and 1:2 were nominated as ZC00, ZC10, ZC11, and ZC12, respectively. The total amount of Zr and C additives in ZC11 and ZC12 was 10 wt% and 11.04 wt%, respectively. The compacts were hot pressed at temperatures ranging from 1800 °C to 2000 °C at intervals of 100 °C for 1 h, with a heating rate of 10 °C/min, under a pressure of 30 MPa. During the hot-pressing process, the samples were heated in a mild vacuum (~10 Pa) to 1450 °C before reaching to soaking temperature under a flowing Ar. From 1450 °C, the load was applied and the punch displacement was recorded automatically to reflect the shrinkage degree of sample during hot pressing sintering. After sintering, the furnace was cooled down to 1700 °C at a rate of 30 °C/min, then naturally to room temperature. The oxygen content measurement of ZrC powder was carried out by Oxygen-Azote menstruation equipment (TC600, LECO, USA). The Zr and C element content in ZC10 and ZC11 were obtained by using chemical analysis technique, in which ethylenediamine tetraacetic acid (EDTA) titration and non-aqueous titration after high temperature combustion were used to measure the amount of Zr and C, respectively.

Table 1
Designation and raw material compositions used in the present work.

Sample	Raw material compositions (wt%)			Molar ratio of additives Zr/C
	ZrC	Zr	C	
ZC00	100	0	0	–
ZC10	91.06	8.94	0	–
ZC11	90	8.84	1.16	1:1
ZC12	88.96	8.74	2.30	1:2

The bulk densities of the specimens were measured using Archimedes' principle. As the major phase of the sintered samples with additive was non-stoichiometric ZrC_{1-x} (see discussion in Sections 3.1 and 3.2), the theoretical densities were obtained based on the calculated densities of ZrC_{1-x} provided by JCPDS cards. The phase identification of sintered samples was made by X-ray diffraction analysis (XRD, D/Max 2550V, Japan). The lattice parameters were determined by X-ray diffractometry using a Guinier-Hägg camera (XDC1000, Sweden) with $CuK_{\alpha 1}$ ($\lambda = 1.5405981$ Å) radiation and Si powder was used as the internal standard. Fracture surfaces of the hot pressed specimens were examined by scanning electron microscopy (SEM, Hitachi S-570, Tokyo, Japan). Microhardness of the samples was measured using Vickers' indentation technique by applying a load of 9.8 N with a dwell time of 15 s. At least 5 indentations were performed to obtain the average hardness value and the standard deviation. The fracture toughness was calculated according to the Evans's equation (1).[21]

$$K_{Ic} = P\left(\pi\left(\frac{C_1 + C_2}{4}\right)\right)^{-3/2}(tg\beta)^{-1} \quad (1)$$

in which P is the peak load (9.8 N), C_1, C_2 are the measured diagonal crack lengths (m) and β is a constant of angle (68°).

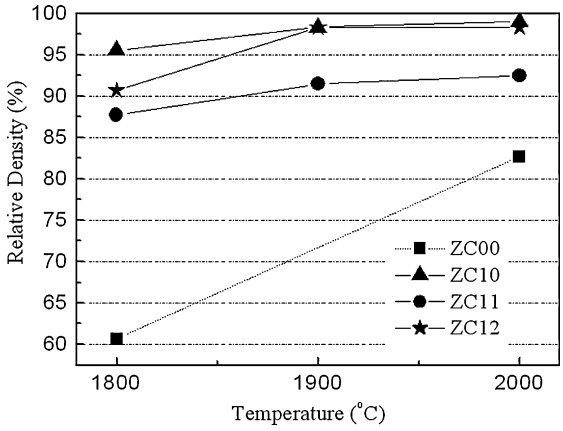

Fig. 1. The relative density as a function of sintering temperature for ZrC samples with and without sintering additives.

3. Results and discussion

The relative densities of ZrC samples without additives as a function of sintering temperatures are shown in Fig. 1. It can be seen that the relative densities of additive-free ZC00 is only 83% even sintered at 2000 °C. The lattice parameter *a* of ZrC phase in raw powders was 4.6948 Å, while it decreased to 4.6932 Å when the ZrC sample was sintered at 2000 °C (see Fig. 2). A possible reason of the decrease in lattice parameter was the formation of HfC or solid solution containing Hf since the raw ZrC powders contain about 3 wt% Hf impurities. According to the densification curve of ZrC (Fig. 1), the densities are mainly affected by sintering temperature and the effect of impurities on densification improvement of ZrC is limited. In order to improve the densification, Zr additive or the combination of Zr and C additives were introduced into ZrC.

3.1. The densification behavior of ZrC with Zr additives

XRD pattern of ZC10 sintered at 1800 °C is shown in Fig. 3a, in which only ZrC phase is detected. The measured lattice parameter of ZrC phase in ZC10 sintered at 1800 °C is 4.6863 Å (see Fig. 2), which is much smaller than that of the ZrC raw powder (4.6948 Å). From phase diagram of the Zr–C system[22] in

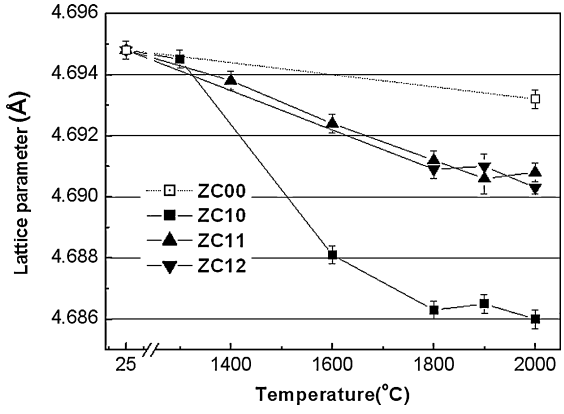

Fig. 2. The lattice parameters variation of ZrC phase in ZC10 vs. sintering temperature.

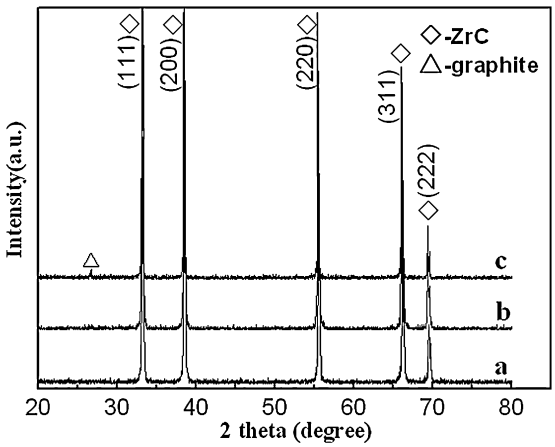

Fig. 3. XRD patterns of ZC10 sintered at 1800 °C (a), ZC11 sintered at 2000 °C (b) and ZC12 sintered at 2000 °C (c).

Fig. 4, it is found that ZrC phase exists when the molar ratios of C to Zr are around in the range from 0.61:1 to 1:1 at 500 °C. Non-stoichiometric ZrC_{1-x} could be formed in the Zr–C binary system. Therefore, it was thought in the present case that the Zr additive would react with ZrC to form non-stoichiometric ZrC_{1-x} in ZC10 sample according to following reaction Eq. (2).

$$(1-x)\mathrm{ZrC} + x\mathrm{Zr} \rightarrow \mathrm{ZrC}_{1-x} \quad (2)$$

It was reported in the literature that the lattice parameter *a* of ZrC_{1-x} decreased from 4.694 Å for $x = 0$–4.680 Å for $x = 0.35$.[15] Therefore, the decrease in lattice parameter of ZrC phase in ZC10 sample implies the formation of non-stoichiometric ZrC_{1-x} according to reaction (2), in which the *x* value would be around 0.1 according to the raw material compositions used in ZC10. The molar ratio of C/Zr measured by chemical analysis technique in ZC10 sintered at 1900 °C was 0.9, which was well consistent with the discussion mentioned above. Therefore, the formula of the final product of ZC10 sintered at 1900 °C would be $ZrC_{0.9}$.

For exploring interactions between ZrC and Zr additive during the sintering processes, ZC10 samples were heated to 1150 °C and 1300 °C at a rate of 10 °C/min without holding time. The phase compositions of the products were identified by XRD method as shown in Fig. 5 in which the XRD patterns of the

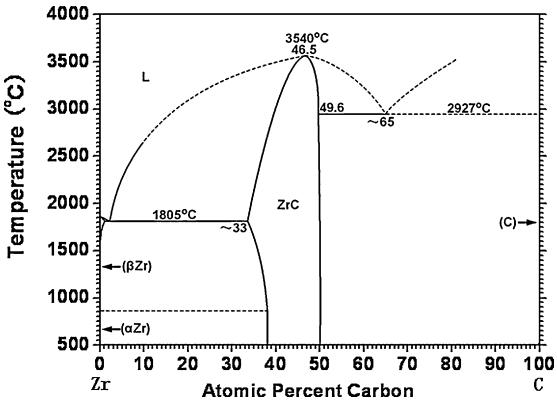

Fig. 4. Phase diagram of Zr–C binary system.[22]

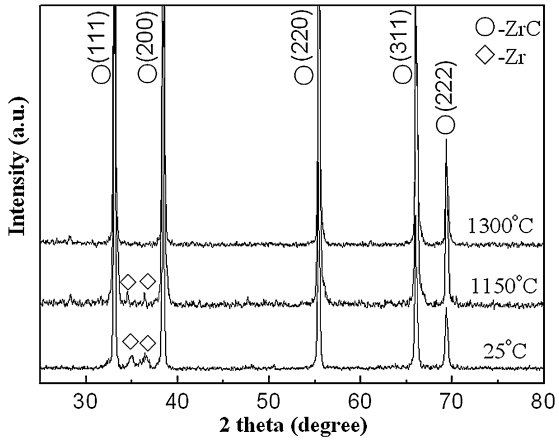

Fig. 5. XRD patterns of ZC10 specimens before and after heating at 1150 °C and 1300 °C.

starting powders (25 °C) is also put for comparison. The width Zr peak at 25 °C is noticeably large, which could be caused by the strain after ball milling.[16] It can be seen that un-reacted Zr is detected at 1150 °C and its XRD peak disappears at 1300 °C, implying that the reaction between ZrC and Zr started in this temperature range. In order to confirm the formation of ZrC_{1-x}, the variation of lattice parameters of ZrC in ZC10 sintered at different temperatures were measured and are shown in Fig. 2. It is found that the lattice parameter a of ZrC in ZC10 decreases with increase in sintering temperature, especially at the temperature range from 1300 °C to 1800 °C, which could be resulted from the formation of ZrC_{1-x}. The above analysis indicates that the formation of non-stoichiometric ZrC_{1-x} occurs mostly in the temperature range of 1300–1800 °C, since the lattice parameter of ZrC_{1-x} keeps more or less constant even further increase in temperature up to 2000 °C. Fig. 6 illustrates the profiles of the strongest XRD peak (2θ is around 33°) of ZrC phase for ZrC raw powder, ZC10 samples sintered at 1150 °C, 1300 °C, and 1600 °C. It can be seen that the XRD peak positions of raw ZrC, ZC10 sintered at 1150 °C and 1300 °C are very close, whereas that of ZC10 sintered at 1600 °C shifts to higher 2θ obviously. It is also noted that there are small satellite peaks appearing on the right of the main peak at 1150 °C and 1300 °C (see arrows indicated in Fig. 6). It is presumed that the small satellite peaks

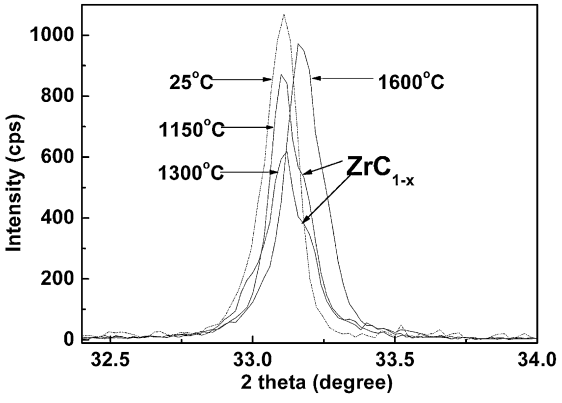

Fig. 6. Expanded XRD peaks of ZC10 samples sintered at different temperatures showing the shift of peaks.

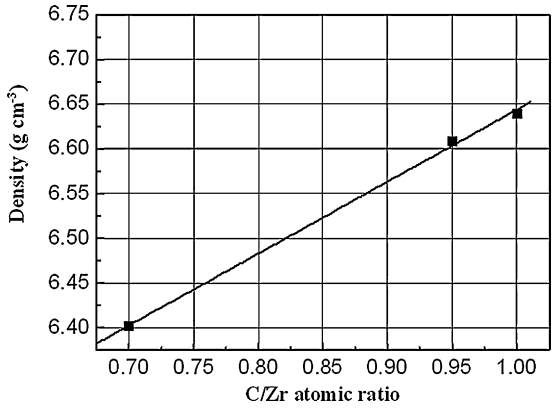

Fig. 7. The fitting curve of theoretical density of ZrC data resulted from JCPDS cards (see text).

are caused by the formation of ZrC_{1-x} and the profile of the XRD peak is resulted from a mixture of stoichiometric ZrC and non-stoichiometric ZrC_{1-x}. The changes in peaks profile and position showed the composition at low temperature (<1600 °C) was non-homogeneous, and ZrC grains generally have a gradient in carbon content with a concomitant variation.[17]

As there was no calculated density data available in JCPDS card for $ZrC_{0.9}$, a linear curve to fit the theoretical densities of ZrC, $ZrC_{0.7}$, and $ZrC_{0.95}$ provided by JCPDS cards was made, as shown in Fig. 7, from which the theoretical density of $ZrC_{0.9}$ could be estimated when a linear relationship between theoretical density of ZrC_{1-x} and the ratio of C to Zr was assumed. It was found that the relative density of ZC10 sintered at 1900 °C reached 98.4%. The results indicated that the addition of Zr greatly improved the densification of ZrC. Meanwhile, in order to make sure the high relative density of ZC10, the polished surface of ZC10 before and after acid etching were prepared and shown in Fig. 8, from which it can be seen the sample was dense with some amount of micropores in the grains.

According to the XRD pattern of ZC10 sintered at 1300 °C, the disappearance of Zr peak revealed that Zr phase would not exist or have just very limited amount in ZC10 at 1300 °C and above. Therefore, it was thought that the densification improvement of ZC10 was not caused by the liquid phase sintering. Lattice parameter analysis confirmed that the addition of Zr into ZrC resulted in the formation of non-stoichiometric ZrC_{1-x}. The carbon vacancy in the lattice enhanced the mass transport through solid-state diffusion during sintering.[18,19] It was reported that the activation energy for sintering of ZrC_{1-x} reduced with increase in carbon vacancy content. For example, the activation energy for sintering of ZrC_{1-x} decreases from 37 kcal/mol at $x = 0$–20 kcal/mol at $x = 0.35$.[18] Therefore, the non-stoichiometric $ZrC_{0.9}$ possesses a better densification behavior than that of ZrC as the relative density (98.4%) can be reached when ZC10 is sintered at 1900 °C. The displacement of punch vs. time for ZC10 sintered at 2000 °C is shown in Fig. 10a, it can be found that that the increase of displacement was obvious at temperature above 1600 °C. Meanwhile, enlarged XRD pattern and lattice parameters show that the composition of ZC10 was not homogeneous with stoichiometric ZrC and non-stoichiometric ZrC_{1-x} coexisted. ZC10 samples were

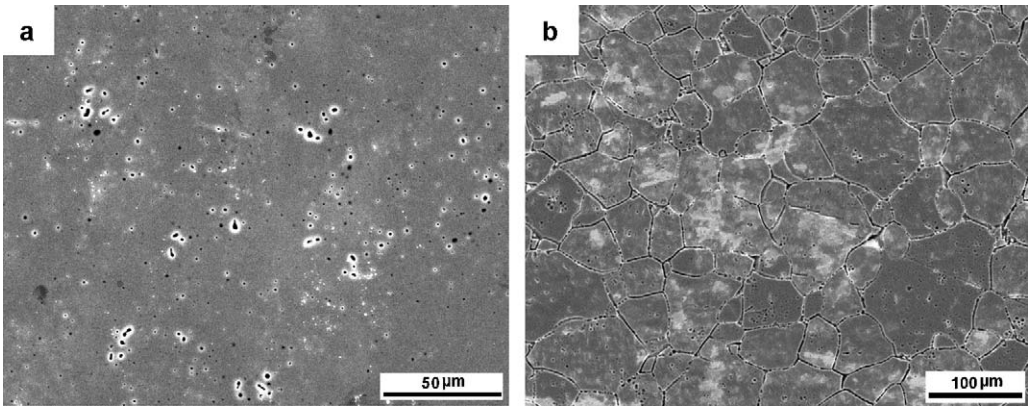

Fig. 8. Polished surface (a) and acid etching surface (b) for ZC10 sample sintered at 2000 °C.

also sintered at 1300 °C and 1600 °C for 1 h, the relative density at 1300 °C and 1600 °C was 54.4% and 78.1%, respectively. So the densification of ZC10 was much depended on temperature. ZC10 cannot be sintered to high relative density below 1800 °C in the present sintering condition.

In addition to carbon-vacancy in ZrC_{1-x} being of advantage to the densification of ZrC, an additional mechanism for densification of non-stoichiometric ZrC_{1-x} is the plastic flow. It was reported that the critical resolved shear stress (CRSS) decreased from about 141 MPa for $TiC_{0.95}$ to 72 MPa for $TiC_{0.83}$.[19] As a member of group IV carbides, ZrC, likes TiC, may also show a falling yield stress with the increase of carbon vacancy concentration. Therefore, the CRRS of $ZrC_{0.9}$ would decrease compared with that of stoichiometric ZrC. During hot pressing, the local stresses around $ZrC_{0.9}$ particle contacts would be considerably higher than the nominal applied stress and can exceed the flow stress, thereby leading to plastic flow and promoting the densification.[19]

3.2. The densification behavior of ZrC with Zr and graphite composite additives

The relative densities of ZC11 samples sintered in the range of 1800–2000 °C (87.7–92.5%) are all higher than those of additive-free ZC00 samples. However, they are lower than that of ZC10 samples sintered at the same temperatures (see Fig. 1). From the displacement of punch vs. time as shown in Fig. 10b, we can also find that the increase rate of displacement of ZC11 was much slower than that of ZC10.

The XRD pattern of ZC11 sintered at 2000 °C is shown in Fig. 3b. Only ZrC phase was identified in ZC11. In order to investigate the detail reaction processes in ZC11, Zr and graphite powder mixtures with the molar ratio of 1:1 were heated to 900 °C, 1150 °C, and 1300 °C at a rate of 10 °C/min without holding time. The XRD patterns of the products after heating are shown in Fig. 9. It can be observed that the intensity of Zr peaks decreased from 900 °C to 1150 °C, and Zr peak disappeared at 1300 °C. Based on the reaction results between Zr and graphite, one can conclude that Zr can reacts with graphite mostly in the range of 1150–1300 °C. Of course, the reaction between Zr and graphite was not complete according to the fact that there is a graphite peak with weak intensity and no Zr peak in XRD pattern as shown in Fig. 9c, implies that the reaction product of zirconium carbide at 1300 °C could be non-stoichiometric ZrC_{1-x} according to reaction (3). Nachiappan et al. reported that the lattice parameter of reaction product between Zr and C mixture (molar ratio 1:1) increased from 4.6876 Å at 1200 °C to 4.6895 Å at 1600 °C, which also revealed that the reaction product was non-stoichiometric ZrC_{1-x} and x value decreased with the increase of temperature.[17] In addition, Zr starts to react with ZrC matrix from 1150 °C to 1300 °C, as mentioned above. Therefore, it could be assumed that Zr may react with both ZrC matrix and graphite in this temperature range. Meanwhile, as an intermediate product, part of ZrC_{1-x} can also react with graphite.

$$Zr + (1-x)C \rightarrow ZrC_{1-x} \quad (3)$$

The measured lattice parameters variation of ZrC phase in ZC10 and ZC11 vs. sintering temperatures is shown in Fig. 2. It is found that lattice parameters of ZrC in ZC10 decrease when sintering temperature increases to 1900 °C. On the other hand, the decrease in lattice parameter of ZrC in ZC11 is much smaller than that in ZC10. For example, at 2000 °C the difference in lattice parameters of ZrC phase between ZC00 and ZC11 samples is about 0.0024 Å, whereas it is more than 0.0072 Å between ZC00 and ZC10. The higher value of ZrC lattice parameters in ZC11 than that in ZC10 is due to that part of Zr reacting

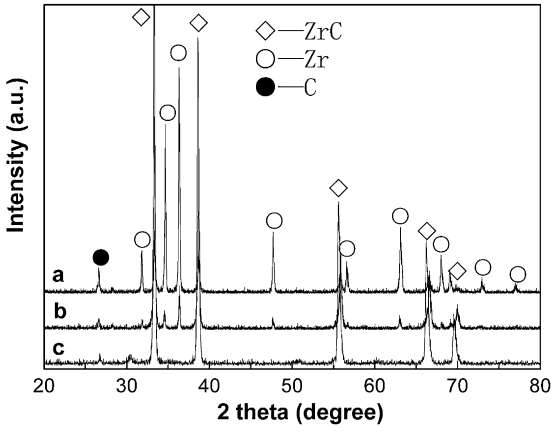

Fig. 9. The XRD patterns of Zr and C mixture heated to (a) 900 °C, (b) 1150 °C and (c) 1300 °C.

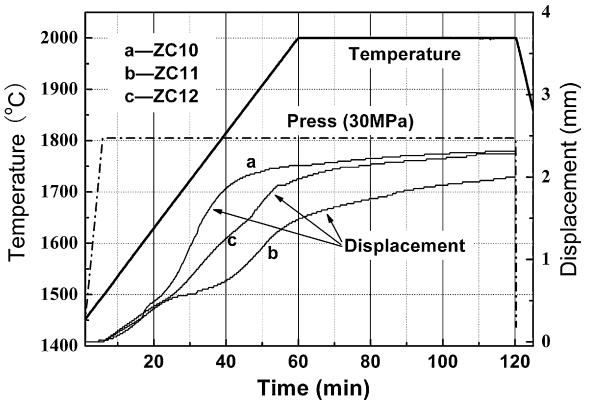

Fig. 10. Displacement of the punch vs. time showing the increase of the shrinkage of sample during hot pressing of material ZC10 (a), ZC11 (b) and ZC12 (c).

with ZrC matrix and the other part of Zr reacting with graphite. As a consequence, the amount of Zr joining in reaction (2) in ZC11 would be less than that in ZC10, resulting in less carbon vacancy in ZC11 compared with that ($ZrC_{0.90}$) in ZC10, i.e. x value of ZrC_{1-x} in ZC11 is lower than that in ZC10. A chemical analysis was also made for ZC11 sintered at 1900 °C and the results showed that the molar ratio of C/Zr was about 0.96. Therefore, the formula of $ZrC_{0.96}$ in ZC11 at temperatures higher than 1800 °C was assumed.

From the above lattice parameter analysis, one can know that part of Zr additive in ZC11 reacted with ZrC matrix forming non-stoichiometric ZrC_{1-x} and the other part of Zr additive reacted with graphite. Although the total addition amount of Zr in the compositions of ZC11 and ZC10 are same, the carbon vacancy concentration in ZC11 was lower than that in ZC10, which caused the difference in densification improvement as shown in displacement plot (Fig. 10b).

It was reported that the presence of oxide impurities on the surfaces of non-oxide ceramics particles of SiC, TaC and ZrB_2 inhibited the densification.[23–25] The oxygen content in as-received ZrC powder was 0.78 wt%. Based on reaction (4), 0.88 wt% graphite was needed to remove all the surface oxide if assuming the oxygen was present in the state of ZrO_2.

$$ZrO_2 + 3C \rightarrow ZrC + 2CO\,(g) \quad (4)$$

In the present work, an additional experiment was conducted to confirm this analysis. First, 0.5 wt% graphite was independently added to ZrC and the result showed that no full densification was obtained at 2000 °C (90.5% relative density), because the added graphite (0.5 wt%) was not enough to remove oxide impurity. Then addition of 1.27 wt% graphite into ZrC was added, which was sintered at 1900 °C and 2000 °C by the same sintering conditions as the first one. The relative densities of as-sintered samples reached 84.5% and 97.7% at 1900 °C and 2000 °C, respectively, revealing that addition of 1.27 wt% graphite did have the effect of removing the oxide impurity and promoted the densification of ZrC ceramics.

As mentioned above, the improved densification of ZC11 in comparison to that of additive free ZC00 was resulted from the formation of $ZrC_{0.96}$. However, the relative density of ZC11 could not be further increased even sintered at 2000 °C (see Fig. 1) because of the formation of less carbon vacancy non-stoichiometric ZrC_{1-x} and limited amount of graphite in ZC11. Therefore, the graphite content was adjusted in ZC12 sample in which the graphite content was increased from 1.16 wt% in ZC11 to 2.30 wt% in ZC12.

The XRD pattern of ZC12 sintered at 2000 °C is shown in Fig. 3c. The result indicates that besides the major phase of ZrC, there is trace amount of graphite. The theoretical density of ZC12 was calculated from the rule of mixtures on the basis of the final phase assemblage. The relative densities of ZC12 are all higher than that of ZC11 sintered at 1800–2000 °C, especially at 1900 °C and 2000 °C (see Fig. 1), which are close to that of ZC10. From the displacement plot (shown in Fig. 10c), it can also be seen that the shrinking rate of ZC12 was much higher than that of ZC11, which is accordance with their relative density data. The polished surface before and after acid etching of ZC12 is shown in Fig. 11, from which flake pores can be seen, this is because that graphite was soft, and graphite phase was easy to flake-off from surface during polishing (Fig. 11a). In addition to the pores caused by the graphite flake-off, trace amount of pores in the grains was also found (Fig. 11b). The lattice parameters of ZrC in ZC12 as shown in Fig. 2, are very close to that in ZC11 ranging from 1800 °C to 2000 °C, which reveals that the similar reactions (Eqs. (2) and (3)) would occur and the final formula of non-stoichiometric ZrC_{1-x} would be $ZrC_{0.96}$ in ZC12 as that

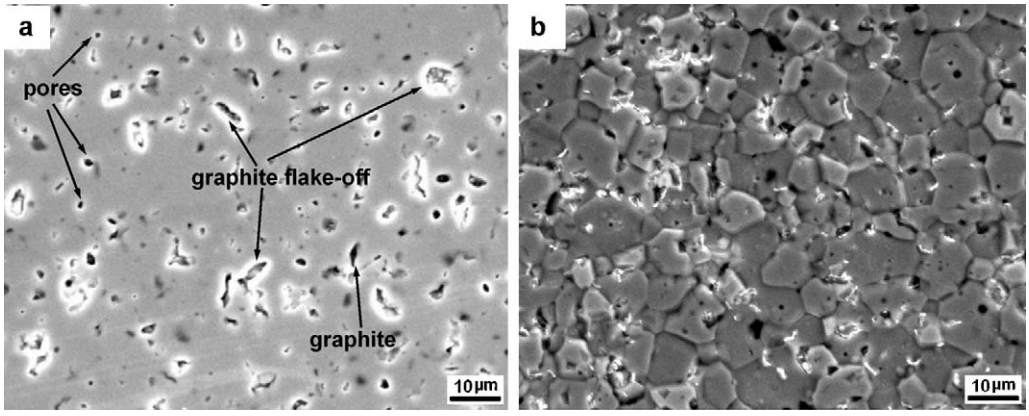

Fig. 11. Polished surface (a) and acid etching surface (b) for ZC12 samples sintered at 2000 °C.

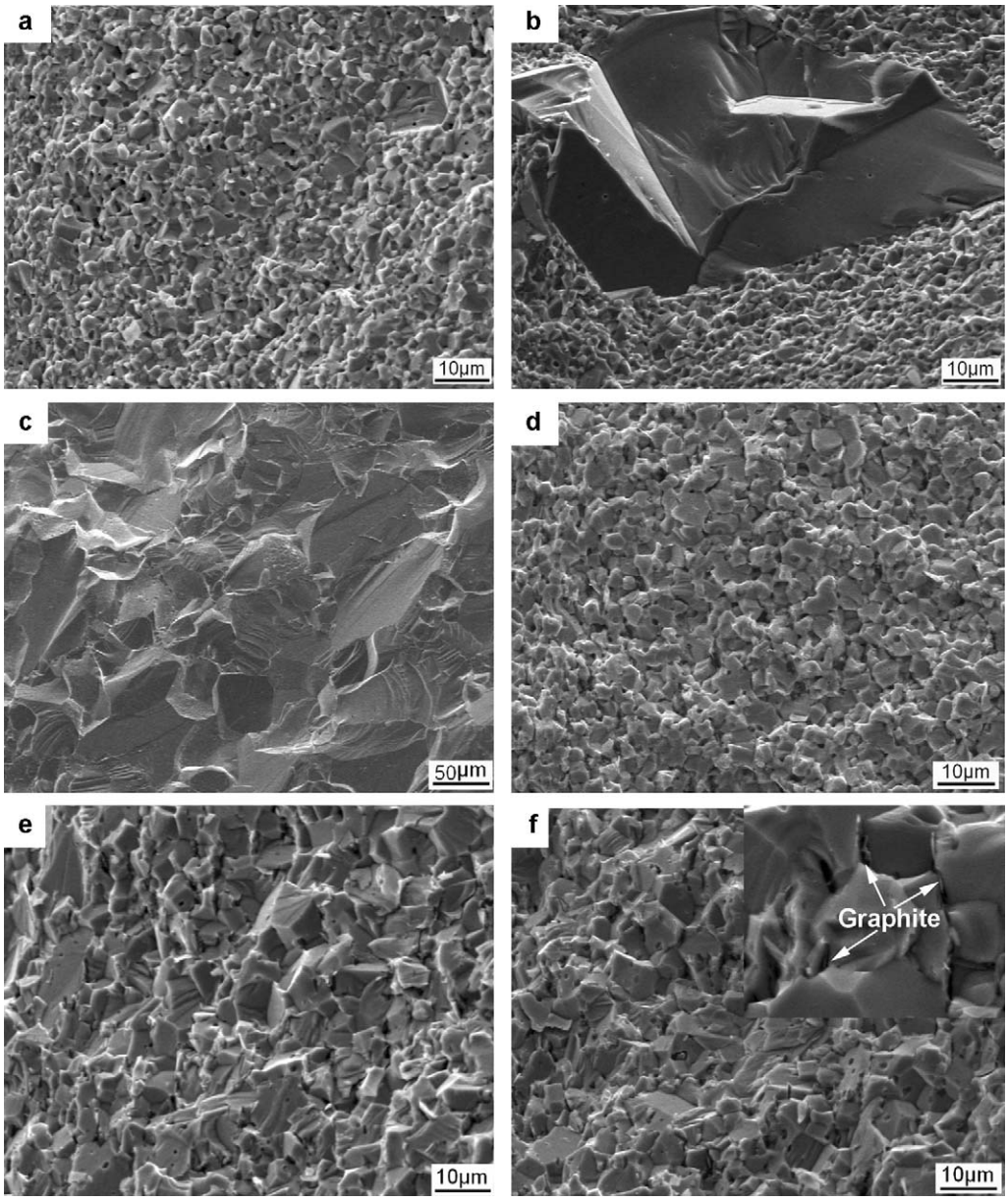

Fig. 12. SEM micrographs of fracture surfaces of the doped samples sintered at different temperatures: (a) ZC10 – 1800 °C, (b) ZC10 – 1900 °C, (c) ZC10 – 2000 °C, (d) ZC12 – 1800 °C, (e) ZC12 – 1900 °C, and (f) ZC12 – 2000 °C. When 8.94 wt% Zr was added, exaggerated grain growth of ZC10 was found at 1900–2000 °C. Inset in (f) shows remnant flake graphite phase.

in ZC11. From the above analysis, it was concluded that by co-doped Zr and graphite additives with Zr/C molar ratio at 1:2 in ZC12 sample, the improved densification is attributed to the combined effects of the formation of non-stoichiometric $ZrC_{0.96}$ and the removal of ZrO_2 impurity.

3.3. The microstructures and mechanical properties of ZrC ceramics with different additives

SEM micrographs of fracture surfaces of ZC10 and ZC12 samples sintered at 1800–2000 °C are shown in Fig. 12. For ZC10 sintered at 1800 °C, the material exhibits a fine microstructure profile with relative density higher than 95%, in which the grain size is around 3–5 μm, as shown in Fig. 12a. However, the exaggerated grain growth (50–100 μm) was observed when ZC10 was sintered at 1900 °C and 2000 °C (see Figs. 12b and c and 8b), which might be resulted from the formation of $ZrC_{0.9}$, which enhances the mass transport and excessive grain growth on the other hand. Pores or voids could generally retard to grain growth. In the present study, the grain growth of ZC10 cannot be inhibited by pores because $ZrC_{0.9}$ has high sinterability at 1900–2000 °C. Therefore, closed pores were found in the grains.

ZC12 shows a fine and stable microstructure with no exaggerated grain growth when sintered at 1800–2000 °C (Figs. 12d–f and 11b) with the grain size of ZrC about 5–10 μm at temperatures from 1900 °C to 2000 °C. The un-reacted graphite tends to place at the grain boundaries as shown in

Table 2
Mechanical properties of ZrC samples doped with different additives and related data.

Sample	Sintering temperature (°C)	Relative density (%)	Vickers hardness (GPa)	Indentation fracture toughness (MPa $m^{1/2}$)
ZC10	1900	98.4	17.8 ± 0.4	3.0 ± 0.8
ZC10	2000	98.9	18.5 ± 0.5	1.9 ± 0.4
ZC11	2000	92.5	12.4 ± 0.2	–[a]
ZC12	1900	98.3	16.2 ± 0.9	4.7 ± 0.4
ZC12	2000	98.2	14.4 ± 0.3	4.0 ± 0.4

[a] Not measured due to the high porosity.

Fig. 12f (inset image), resulting in the decrease of the mean grain size. It was thought that the remnant graphite phase in ZC12 would inhibit the grain growth during sintering. In addition, the low carbon-vacancy concentration of $ZrC_{0.96}$ also had no high promotion to the grain growth.

The mechanical properties of the ZrC samples with different additives are listed in Table 2. The Vickers hardness of ZC10 sintered at 1900 °C is 17.8 GPa, and increases to 18.5 GPa, which is statistically similar to the reported value for monolithic ZrC in the literature.[8] Because of the high porosity of ZC11 (relative density 92.5% at 2000 °C), its Vickers hardness is very low (12.4 GPa). The Vickers hardness of ZC12 (16.2 GPa) is slightly lower in comparison to that of ZC10 (17.8 GPa) sintered at the same temperature (1900 °C), which is attributed to the appearance of remnant graphite phase that is regarded as the source of more severe plastic deformation during the indentation process.[26] The indentation toughness of ZC12 was about 4.7 and 4.0 MPa $m^{1/2}$ sintered at 1900 °C and 2000 °C, respectively, while the fracture toughness of ZC10 decreased from 3.0 MPa $m^{1/2}$ at 1900 °C to 1.9 MPa $m^{1/2}$ at 2000 °C. On the base of microstructure observation, it was found that the fracture modes of ZC12 and ZC10 were mainly intergranular and transgranular, respectively, which could explain the higher value of fracture toughness of ZC12 than that of ZC10.

4. Conclusions

By adding Zr and graphite additives, ZrC ceramics were densified by hot-pressing at temperatures ranging from 1800 °C to 2000 °C, whereas the relative density of additive-free ZrC material sintered at 2000 °C was 83%. Adding Zr additive to ZrC, the improvement in densification of ZC10 was resulted from the formation of non-stoichiometric $ZrC_{0.9}$ by the reaction between ZrC and Zr. There appeared an exaggerated grain growth (50–100 μm) in ZC10 sample at 1900–2000 °C. For Zr and C co-doped samples with the Zr/C molar ratio up to 1:1, the sinterability was lower than that of ZC10 because of less carbon-vacancy concentration. However, the removal of oxide contamination during sintering further favors the densification when excess of graphite is added. The relative density of co-doped ZrC with adjusted Zr/C molar ratio up to 1:2 (ZC12) reached 98.4% when hot-pressed at 1900 °C. Un-reacted C tended to place at the grain boundaries in the case of ZC12, and the sample showed a fine and stable microstructure (grain size about 5–10 μm) at 1900–2000 °C. On the other hand, the presence of soft graphite provoked a decrease of hardness of the material. The Vickers hardness and indentation toughness of ZC10 and ZC12 samples sintered at 1900 °C were 17.8 GPa and 3.0 MPa $m^{1/2}$, 16.2 GPa and 4.7 MPa $m^{1/2}$, respectively.

Acknowledgements

Financial supports from the Chinese Academy of Sciences under the Program for Recruiting Outstanding Overseas Chinese (Hundred Talents Program), the National Natural Science Foundation of China (No. 50632070) are greatly appreciated.

References

1. Opeka MM, Talmy IG, Wuchina EJ, Zaykoski JA, Causey SJ. Mechanical, thermal, and oxidation properties of refractory hafnium and zirconium compounds. *J Eur Ceram Soc* 1999;**19**:2405–14.
2. Upadhya K, Yang JM, Hoffman WP. Materials for ultrahigh temperature structural applications. *Am Ceram Soc Bull* 1997;**76**:51–6.
3. Martienssen W, Warlimont H. *Springer handbook of condensed matter and materials data*. Heidelberg: Springer Berlin; 2005.
4. Wang YG, Liu QM, Liu JL, Zhang LT, Cheng LF. Deposition mechanism for chemical vapor deposition of zirconium carbide coatings. *J Eur Ceram Soc* 2008;**91**:1249–52.
5. Lipke DW, Zhang Y, Liu Y, Church BC, Sandhage KH. Near net-shape/net-dimension ZrC/W-based composites with complex geometries via rapid prototyping and displacive compensation of porosity. *J Eur Ceram Soc* 2010;**30**:2265–77.
6. Gosset D, Dolle M, Simeone D, Baldinozzi G, Thome L. Structural evolution of zirconium carbide under ion irradiation. *J Nucl Mater* 2008;**373**:123–9.
7. Vasudevamurthy G, Knight TW, Roberts E, Adams TM. Laboratory production of zirconium carbide compacts for use in inert matrix fuels. *J Nucl Mater* 2008;**374**:241–7.
8. Sciti D, Guicciardi S, Nygren M. Spark plasma sintering and mechanical behaviour of ZrC-based composites. *Scripta Mater* 2008;**59**:638–41.
9. Goutier F, Trolliard G, Valette S, Maître A, Estournes C. Role of impurities on the spark plasma sintering of ZrC_x–ZrB_2 composites. *J Eur Ceram Soc* 2008;**28**:671–8.
10. Barnier P, Brodhag C, Thevenot F. Hot-presing kinetics of zirconium carbide. *J Mater Sci* 1986;**21**:2547–52.
11. Spivak II, Klimenko VV. Densification kinetics in the hot pressing and recrystallization of carbides. *Powder Metall Met Ceram* 1973;**12**:883–7.
12. Landwehr SE, Hilmas GE, Fahrenholtz WG, Talmy IG. Processing of ZrC–Mo cermets for high-temperature applications, part I: chemical interactions in the ZrC–Mo system. *J Am Ceram Soc* 2007;**90**:1998–2002.
13. Hamjian WG, Lidman HJ. Reactions during sintering of a zirconium carbide–niobium cermet. *J Am Ceram Soc* 1964;**35**:236–40.
14. Min-Haga E, Scott WD. Sintering and mechanical properties of ZrC–ZrO_2 composites. *J Mater Sci* 1988;**23**:2865–70.
15. Chamberlain AL, Fahrenholtz WG, Hilmas GE. Low-temperature densification of zirconium diboride ceramics by reactive hot pressing. *J Am Ceram Soc* 2006;**89**:3638–45.
16. Wu WW, Zhang GJ, Kan YM, Wang PL. Reactive hot pressing of ZrB_2–SiC–ZrC composites at 1600 °C. *J Am Ceram Soc* 2008;**91**:2501–8.
17. Nachiappan C, Rangaraj L, Divakar C, Jayaram V. Synthesis and densification of monolithic zirconium carbide by reactive hot pressing. *J Am Ceram Soc* 2010;**93**:1341–6.

18. Samsonov GV, Koval'chenko MS, Petrykina RY, Naumenko VY. Hot pressing of the transition metals and their carbides in their homogeneity regions. *Powder Metall Met Ceram* 1970;**9**:713–6.
19. Rangaraj L, Suresha SJ, Divakar C, Jayaram V. Low-temperature processing of ZrB_2–ZrC composites by reactive hot pressing. *Metall Mater Trans A* 2008;**39**:1496–505.
20. Dariel MP. Enhanced mass transport in titanium carbide at large departures from stoichiometry. *Powder Metall Met Ceram* 2003;**42**:460–7.
21. Evans AG, Charles EA. Fracture toughness determinations by indentation. *J Am Ceram Soc* 1976;**59**:371–2.
22. Barabash OM, Koval YN. *Crystal Structure of Metals and Alloys*. Kiew: Naukova Dumka; 1986. pp. 215–216 (in Russian).
23. Stobierski L, Gubernat A. Sintering of silicon carbide I. Effect of carbon. *Ceram Int* 2003;**29**:287–92.
24. Zhang XH, Hilmas GE, Fahrenholtz WG, Deason DM. Hot pressing of tantalum carbide with and without sintering additives. *J Am Ceram Soc* 2007;**90**:393–401.
25. Zhu SM, Fahrenholtz WG, Hilmas GE, Zhang SC. Pressureless sintering of zirconium diboride using boron carbide and carbon additions. *J Am Ceram Soc* 2007;**90**:3660–3.
26. Zhu SM, Fahrenholtz WG, Hilmas GE, Zhang SC. Pressureless sintering of carbon-coated zirconium diboride powders. *Mater Sci Eng: A* 2007;**459**:167–71.